Research Article

Received: 3 March 2022 Revised: 4 July 2022 Accepted article published: 11 July 2022 Published online in Wiley Online Library: 27 July 2022

(wileyonlinelibrary.com) DOI 10.1002/ps.7073

Evaluation of macadamia felted coccid (Hemiptera: Eriococcidae) damage and cultivar susceptibility using imagery from a small unmanned aerial vehicle (sUAV), combined with ground truthing

Ishakh Pulakkatu-thodi,[a*] Jason Dzurisin[b] and Peter Follett[a]

Abstract

BACKGROUND: Macadamia felted coccid, *Acanthococcus ioronsidei* (Williams) (Hemiptera: Eriococcidae), is a significant pest of macadamia nut, *Macadamia integrifolia* Maiden & Betche (Protaceae), in Hawaii, and heavy infestations can kill branches, resulting in characteristic dead, copper-colored leaves. Small Unmanned Aerial Vehicles (sUAV) or 'drones,' combined with spatial data analysis, can provide growers with accurate and high-resolution detection of plant stress due to pest infestations. We investigated the feasibility of using RGB (red-green-blue) color images from sUAV to detect dieback caused by macadamia felted coccid infestation and compared sUAV estimates with ground-based damage estimates (ground truthing).

RESULTS: Spatial analysis showed clustering of foliar damage that reflected cultivar susceptibility to macadamia felted coccid infestation, with cultivars 344 and 856 being susceptible, and cultivars 800 and 333 being tolerant. sUAV and ground-based estimates of foliar damage were similar for the cultivar 344, but ground-based assessments were higher than sUAV for cultivar 856, possibly due to the differences in canopy architecture and significant early dieback in the lower canopy. At foliar damage levels <10%, sUAV and ground truthing data were significantly positively correlated, suggesting sUAV may be useful in detecting early stages of macadamia felted coccid infestation.

CONCLUSIONS: Cultivars showed varying susceptibility to macadamia felted coccid infestation and the foliage damage appeared in clusters. sUAV was able to detect the foliage damage under high and low infestation scenarios suggesting that it can be effectively used for the early detection of infestations.

Keywords: macadamia felted coccid; Eriococcidae; Hawaii; drones

1 INTRODUCTION

The use of small Unmanned Aerial Vehicles (sUAV) or 'drones' in agriculture is changing farming practices and the management of agricultural resources worldwide. Potential applications of drones in agriculture include surveillance and monitoring for the detection of plant diseases[1] and pest outbreaks,[2,3] precision-mapping of agricultural lands for weed management,[4] assessment of soil and plant fertility,[5] and delivering intervention measures, such as pesticide sprays,[6–9] and release of biological control agents[10] or sterile insects.[11,12] For agricultural surveillance and monitoring, sUAV equipped with multispectral cameras and sensors acquire high-resolution aerial imagery which are post-processed using deep learning algorithms.[2,13] Canopy-level characterization of disease or pest incidence is made possible by processing various vegetation indices extracted from the hyperspectral, multispectral, or RGB imagery.[2] For surveillance of crop damage or plant stress, drones offer unparalleled situational awareness for field applications by providing data with very high temporal and spatial resolution. In forest and tree crops, drones are particularly useful where canopies are inaccessible to ground-based observers.

Often, crop-specific use of drones for field applications requires characterization and standardization of crop-specific spectral responses. There have been a range of studies in annual agricultural crops using sUAV data to characterize spectral responses

* *Correspondence to: I Pulakkatu-thodi, USDA-ARS Daniel K. Inouye U.S. Pacific Basin Agricultural Research Center, 64 Nowelo St, Hilo, HI 96720, E-mail: ishakpt@gmail.com*

a *USDA-ARS Daniel K. Inouye U.S. Pacific Basin Agricultural Research Center, Hilo, HI, USA*

b *Colorado State University, Fort Collins, CO, USA*

for various applications. In soybean, sUAV-collected data have been used to estimate plant height,[14] characterize drought stress,[15] classify pest incidence,[2] and predict yield.[16,17] Similar studies have been conducted in wheat,[18–20] corn,[21,22] and cotton.[23,24] In perennial tree crops such as apples and avocados, sUAV-based hyperspectral imagery has been used for disease monitoring and yield estimation.[25–27] Previous efforts to study canopy stress due to diseases or pests in forest crops using sUAV have shown promising results. In radiata pine trees, *Pinus radiata* D. Don, needle discoloration and early stages of stress development could be identified using multi-spectral imagery collected by sUAV.[28] Hyperspectral data acquired using a sUAV to detect European spruce bark beetle (*Ips typographus* L.) infestations in Norway spruce (*Picea abies* L. Karst.) were used to classify the trees as healthy, infested, or dead.[29] Similarly, differences in spectral signatures acquired by sUAV were used to characterize defoliation of oak trees (*Quercus* sp.) caused by oak splendour beetle (*Agrilus biguttatus* Fabricius).[30]

Hawaii is the primary producer of macadamia nuts, *Macadamia integrifolia* Maiden & Betche (Proteaceae), in the United States, with 7300 ha producing nuts with an estimated farm gate value of $54 million in 2017–2018.[31] Macadamia nut trees can grow to 8 m, and dense plantings can result in overlapping canopies that facilitate the spread of pests within orchards. Tree height and dense canopies can also make application of insecticides difficult and costly. Over 90% of macadamia orchards are >4 ha, but >80% of Hawaii's production occurs on large farms that are >1000 ha. Macadamia felted coccid *Acanthococcus* (previously *Eriococcus*) *ironsidei* (Williams) (Hemiptera: Eriococcidae) is an invasive pest of macadamia nut trees in Hawaii that causes significant crop loss. Macadamia felted coccid is a small, sap-feeding insect; immature and adult life stages can infest all the above-ground parts of the tree, including the trunk, branches, racemes, and fruits.[32] Early infestations of macadamia felted coccid often go unnoticed because of the inconspicuous nature of the pest and practical difficulties associated with manually scouting large orchards. Heavy infestations can kill whole branches, resulting in characteristic dead, copper-colored leaves. At present, macadamia felted coccid populations are quantified by counting the number of crawler-stage insects per unit area of the bark of infested trees[33]. Field scouts use coarse-grit sandpaper to smooth out the rough bark on a selected area of a branch or the main trunk then wrap double-sided sticky tape around the sanded area which captures moving crawlers for monitoring. This type of active monitoring by scouts, while accurate and reliable, has its limitations. The process is time-consuming and has limited scope in large orchards that span hundreds of hectares. Because the injury caused by the macadamia felted coccid manifests as die-back of branches with characteristic copper-colored foliage, alternative approaches such as the use of unmanned aerial vehicles (sUAV) and image classification could be used for pest surveillance and damage estimation.

Typically, many macadamia cultivars are inter-planted in orchards to aid in cross-pollination or as a replacement for dead or declining trees, and growers have observed differences in susceptibility to macadamia coccid infestations among cultivars.[34] In orchards with high-density planting, adjacent canopies often overlap and aid in the spread of macadamia felted coccid within an orchard. Distribution of cultivars with varying levels of susceptibility within the orchard might, therefore, influence the pattern of macadamia felted coccid infestation. Predictability in the pattern of infestation can facilitate site-specific management in existing orchards by directing management resources such as the application of insecticides to the area most in need, which in turn can help to reduce management costs. For macadamia felted coccid, the only mobile life stages are wingless crawlers (all instars) and winged adult males, and the spread of the pest within the field might be influenced by the planting layout of tolerant and susceptible cultivars.

As part of ongoing efforts to manage macadamia felted coccid in macadamia orchards in Hawaii efficiently, reliable methods for the detection and characterization of macadamia felted coccid infestations are needed. Drone-based pest detection would be advantageous in macadamia orchards because of greater ability to sample tree canopies and view trees growing on steep or rocky terrain. The objectives of this study were to (i) investigate the feasibility of using sUAV images to evaluate macadamia felted coccid infestation and damage levels in comparison to ground-based damage estimates ('ground truthing') and (ii) assess differences in susceptibility of macadamia nut cultivars to felted coccid infestation and damage.

2 MATERIALS AND METHODS

2.1 Description of sampled orchards

The study was conducted in 2020 at a commercial macadamia plantation (MacFarms of Hawaii) in South Kona on Hawaii Island. Three blocks of macadamia trees were identified that showed signs of macadamia felted coccid infestation based on visible foliar damage. The research blocks had received standard agronomic care, including irrigation and fertilization, consistent with the orchard management program of MacFarms of Hawaii. All three blocks had more than one cultivar interplanted in varying patterns. Block 1 (19°09′28.7″N 155°51′34.2″W) had cultivar 344 planted in sets of five rows followed by one or two rows of cultivar 800, with a spacing of approximately 4.5 m among trees within a row and 9.5 m between rows. The block consisted of 265 trees of cultivar 344 and 69 trees of cultivar 800 planted in 14 rows. Out of the 14 rows, 11 rows were planted entirely with cultivar 344 and the remaining three rows were planted mostly with cultivar 800 except for three trees of 344 which were planted as replacements for lost trees (Fig. 1(A)).

Block 2 (19°09′28.7″N 155°51′34.2″W) originally included only cultivar 333 but was later interplanted with cultivar 856 to increase the planting density and replace any original trees that had been lost due to diseases or other factors. The final spacing between trees within rows was about 4.5 m and 9.5 m between rows. The block had 142 trees of cultivar 333 and 181 trees of cultivar 856, planted in 14 rows in an alternating pattern except in some areas where there had been heavy losses of trees from the original planting (Fig. 1(B)). Two other cultivars (246 and 344) were also present in limited numbers (4 and 8 trees, respectively) and were not included in the analysis (Fig. 1(B)). A few trees of cultivar 333 in block 2 showed signs of 'slow decline,' an unrelated disease caused by *Kretzschmaria clavus* (Fr.) Sacc. that is characterized by yellowing of leaves and defoliation.[35] This damage was easily distinguished from macadamia felted coccid damage because infected branches were mostly bare or had yellowish leaves. In Block 3 (19°09′21.5″N 155°51′09.0″W), cultivar 333 was the major cultivar with a total of 256 trees, followed by cultivar 508, of which 56 trees were planted in no specific pattern in 13 rows (Fig. 1(C)). Blocks 1 and 2 had been sprayed with horticultural oil and an insect growth regulator 2 weeks before the start of the study to control macadamia felted coccid.

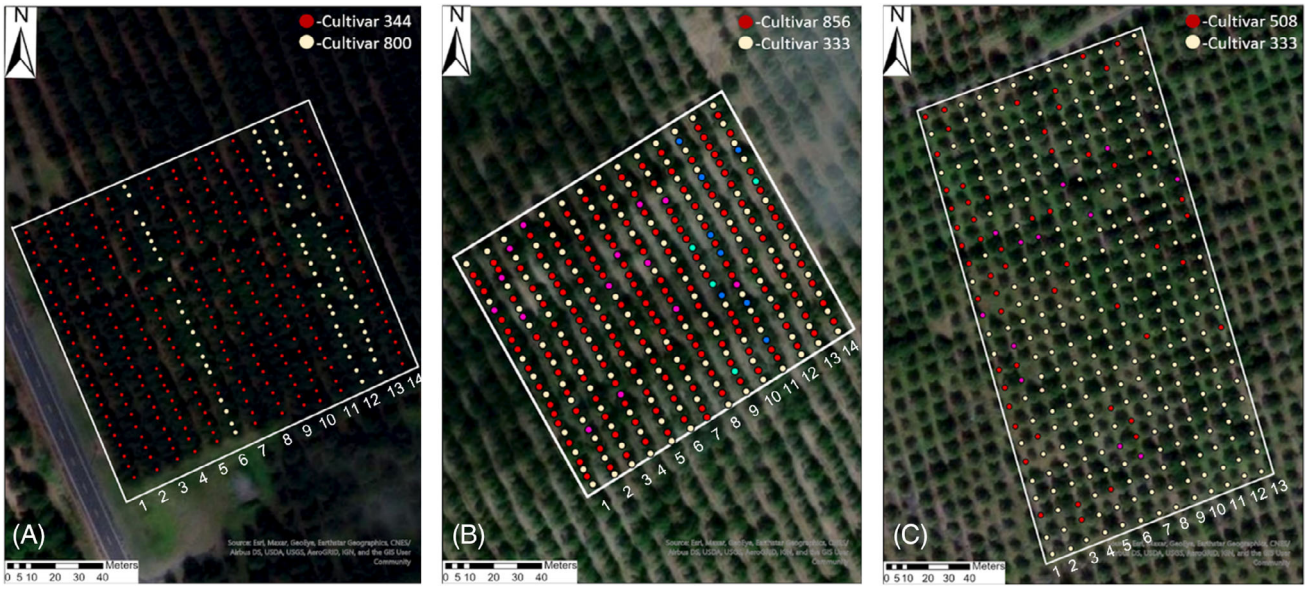

Figure 1. (A) Block 1, (B) block 2, and (C) block 3, each showing block boundaries and planting layout of major cultivars. Different cultivars are marked with red or white dots, while missing trees are denoted by blue dots.

2.2 Ground-based assessment of macadamia felted coccid damage

From each block, 25 trees from each of 13 or 14 rows were selected for sampling or observation (Fig. 1). The location and variety of each tree was recorded using a handheld GPS device (Juno, Trimble, USA). To assess the macadamia felted coccid damage on these trees, individual tree canopies were visually divided into four vertical quarters - two quarters each from opposing sides of the trees looking at a 90° angle from the alleyways.[28] The primary observation, foliar damage, was visually assessed as percent foliar damage for each of the four sampled quarters. These four values were averaged to obtain a mean percent foliar damage for each tree. To confirm the presence of macadamia felted coccid on the macadamia trees, a macadamia felted coccid count was taken from every fourth tree in each row from block 1 (88 trees) and from every tree on alternate rows in block 2 (157 trees). These macadamia felted coccid counts was taken from 6.45 cm^2 (1 in^2) of bark from the main trunk or a lateral branch of each tree. The counts were based on the dead remains of macadamia felted coccid adults. Counting of macadamia felted coccid from the block 3 was not attempted because the macadamia felted coccid remains were in an advanced state of decomposition.

2.3 Aerial assessment of macadamia felted coccid damage

Aerial assessment of macadamia felted coccid using drones was done using a small, commercially available, multirotor sUAV (DJI Phantom 4 Pro). In each block, images were taken from a constant altitude of 60 m in a single grid pattern (Fig. 2). Twenty-megapixel RGB (red-green-blue)-color images were captured with an overlap and sidelap (encompasses the overlapping areas of photographs between adjacent flight paths) of 85%. Images were processed with Pix4DMapper 4.5.2 (Pix4D SA, Prilly, Switzerland) to create a single RGB orthoimage (as a .tif file) and a point cloud (as a .las file) per block. The resolution or the Ground Sampling Distance of the resultant orthoimages was approximately 1.5 cm per pixel.

The RGB orthoimages were imported to ArcGIS Pro 2.6 (ESRI, Redlands, CA, USA) for damage classification (Fig. 3). From these orthoimages of each block, between 15 and 25 sample patches were identified as training data sets for classifying healthy foliage, macadamia felted coccid-damaged foliage, and dead wood. To identify sample patches of macadamia felted coccid damage, we relied on the characteristic copper-colored leaves visible from the imagery. Healthy sample patches were identified from visually healthy areas (green foliage) of the canopy where foliar damage was absent. Dead branches were identified based on lack of foliage and grey appearance of bare branches. A Support Vector Machine algorithm was trained and applied to classify each pixel into one of the above three categories. The Support Vector

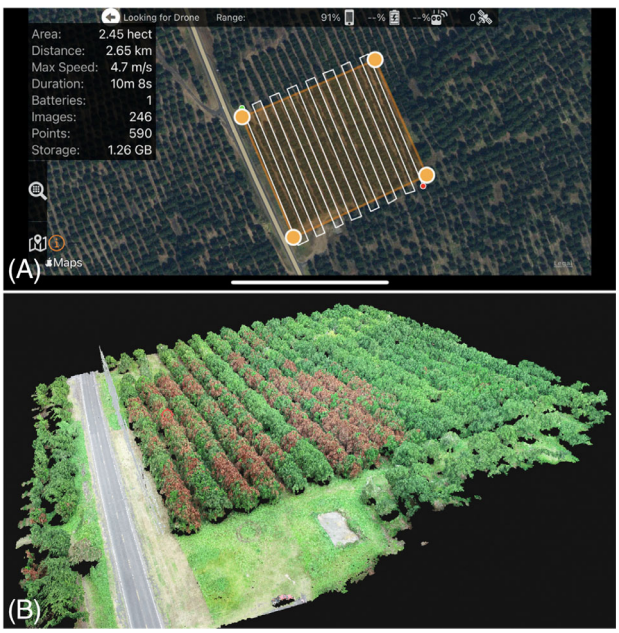

Figure 2. (A) Representative image showing sUAV mapping flight path and (B) a point cloud generated using sUAV imagery of macadamia trees damaged by macadamia felted coccids in Hawaii.

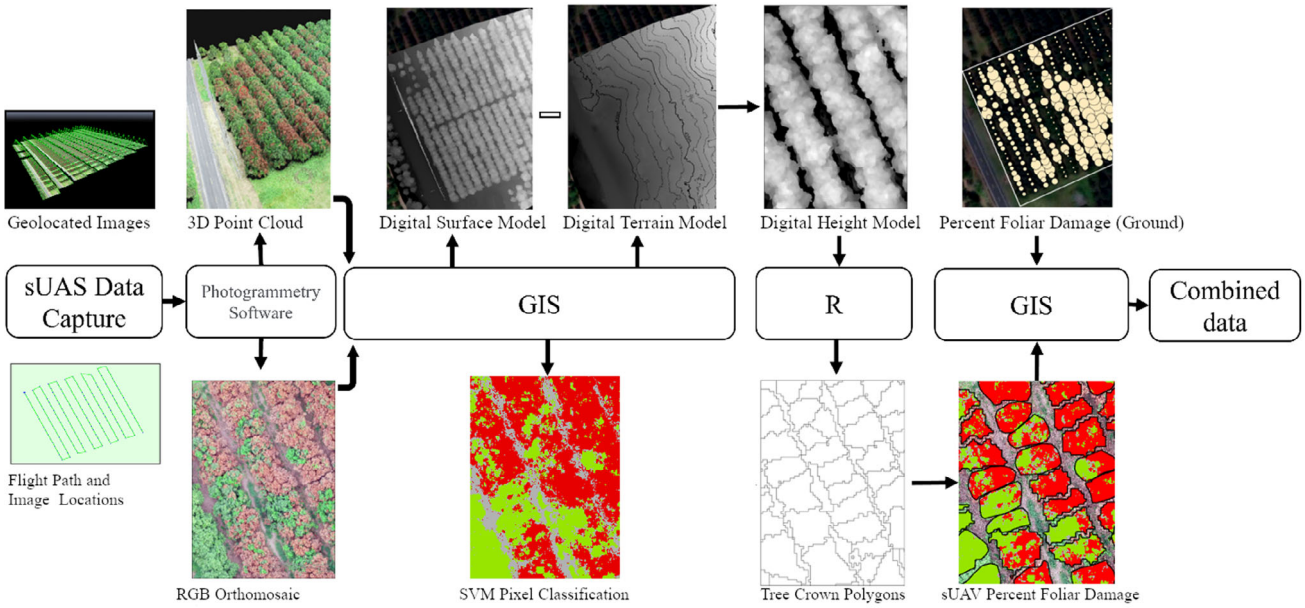

Figure 3. A simplified infographic detailing major steps in aerial data acquisition, image processing, and combining of aerial and ground data.

Machine algorithm was selected because of its low susceptibility to noise (non-target pixels), correlated bands (visually and numerically similar), and unbalanced training sample sizes.

The point cloud dataset was imported into ArcGIS Pro, and images were classified to separate vegetation (*i.e.*, non-ground returns) from ground returns (Fig. 3). From each classified point cloud, a Digital Surface Model and a Digital Terrain Model were generated. A Canopy Height Model, which represents elevation values in meters, was created by subtracting the Digital Terrain Model values from the Digital Surface Model values. From the Canopy Height Model, individual tree crowns and crown centers were automatically identified and delineated using R[36] and the package Forest Tools, which employs a Variable Window Filter[37] to identify local elevation maxima, which represent the center of each tree's crown. Once crown tops were identified, a Marker-Controlled Watershed Segmentation algorithm was run on the dataset for each of those identified crown tops to outline the extent of the crown based on the local minima. The generated crowns were imported into ArcGIS Pro and used to clip the classified RGB orthoimage to isolate tree canopy data and associate each such image with a unique tree ID. Classified pixel counts were used to calculate the percentage of damaged pixels per crown for comparison to ground-based detection methods. Geographic coordinates of individual trees, varietal information, and coordinates of the field boundaries were imported to ArcGIS and spatially joined to the ground assessment data *via* the GPS locations to generate pairs of damage scores tied to each tree.

2.4 Data analysis

Parametric and non-parametric statistical tests were used to analyze percent foliar damage data from ground-based assessments. Specifically, we used a Wilcoxon two sample t-test to compare differences between cultivars. For the same dataset, we used the PROC GLIMMIX procedure[38] to compare the mean percent damage among rows. To visualize ground-based damage assessment scores, spatial data visualization tools such as a proportional bubble map and Inverse Distance Weighted interpolation map were used.[39,40] A proportional bubble map was used to visualize raw data, while we used Inverse Distance Weighted interpolation map after assigning a spatial weight based on the distances between trees. Moran's *I* was used for statistical hypothesis testing of the spatial distribution of infestation. This index evaluates the observed data based on tree locations and describes the spatial distribution as clustered, dispersed, or random.[41] The PROC REG procedure[38] was used to compare ground-based and sUAV assessments.

3 RESULTS

3.1 Ground-based assessment of macadamia felted coccid damage among different cultivars

For block 1, the average percent foliar damage was 24.64 ± 1.5 (n = 334). The two cultivars had significant different levels of foliar damage (Wilcoxon test: $Z = -11.23$, $P < 0.01$). A total of 86.4% (229 trees) of cultivar 344 showed some level of foliar damage, while no trees of cultivar 800 showed any damage. The range of percent foliar damage per tree for cultivar 344 was 0–90%, with a mean of 31.00 ± 1.6. Significant variation of foliar damage among rows was detected in block 1 ($F = 21.18$; $df = 13, 320$; $P < 0.01$; Table 1). Rows in the middle (Fig. 4(A)) had the highest level of foliar damage, ranging from 47.0 ± 0.1 to 54.3 ± 0.0%. Row 6, which consisted of mostly cultivar 800, exhibited no signs of infestation despite being located between two heavily infested rows of cultivar 344, suggesting tolerance in cultivar 800 against the macadamia felted coccid. This trend was also seen in row 6, where two trees of cultivar 344 had been interplanted that were infested with macadamia felted coccid but did not appear to spread macadamia felted coccid to the nearby cultivar 800 trees. From the trees that were sampled for macadamia felted coccid count (n = 88) in block 1, cultivar 344 had a mean macadamia felted coccid count of 57.47 ± 9.3 per 6.45 cm^2 of bark (n = 70) and cultivar 800 had a mean macadamia felted coccid count 8.77 ± 7.4 per 6.45 cm2 of bark (n = 18).

The block 2 had an overall foliar damage of 2.4 ± 0.4% (n = 323). A total of 75 out of 181 trees (41.4%) of the cultivar 856 exhibited some degree of foliar damage, while no trees of cultivar 333 showed damage. For cultivar 856 (n = 181), the range of foliar damage was 0–62.5 ± 0.7%, with a mean of 4.42 ± 0.7%. The two cultivars differed significantly in percent foliar damage levels (Wilcoxon test: Z = -8.63; $P < 0.01$). Row identity was a significant factor affecting the level of foliar damage (F = 4.87; df = 13, 309; $P < 0.01$; Table 1). The first three rows on the northeast side of the block and the seven rows on the southwest side had two or more trees with foliar damage within each row (Fig. 4(B)). The remaining rows in the middle of block 2 had no damaged trees, indicating two separate clusters of macadamia felted coccid infestation.

Macadamia felted coccid population estimates from bark infestations were collected from 157 trees consisting of both cultivars from block 2. Of these trees, cultivar 856 had a mean macadamia felted coccid count of 58.39 ± 12.1 per 6.45 cm^2 of bark (n = 88) and cultivar 333 had a mean macadamia felted coccid count of 0.43 ± 0.4 per 6.45 cm^2 of bark (n = 69). Macadamia felted coccid counts were collected from block 1 and block 2 to confirm the presence of macadamia felted coccid in the sampled blocks. Because the counting was based on dead remains after an insecticidal spray, statistical analysis on the count data was not attempted.

In block 3, of the 56 trees of cultivar 508, 48 (85.7%) had symptoms of foliar damage from macadamia felted coccid, but only 6 trees out of 256 (0.02%) of cultivar 333 showed symptoms of macadamia felted coccid. Cultivar 508 had the higher level of foliar damage at 11.53 ± 1.8%, while that of cultivar 333 was 0.30 ± 0.2%. Overall, the percent foliar damage in block 3 (for both varieties) was 2.31 ± 0.4, which was substantially lower than in block 1 and comparable to block 2. Cultivars differed significantly in mean percent foliar damage using a Wilcoxon two sample t-test (Z = −14.95; $P < 0.01$). Percent foliar damage also differed significantly among rows (F = 4.54; df = 12, 300; $P < 0.01$; Table 1). The rows with highest damage were concentrated near the western side of the block where cultivar 508 was clustered (Fig. 4(C)).

3.2 Spatial analysis

In block 1, spatial mapping of the percent foliar damage by tree showed a clear pattern of infestation confined to cultivar 344 (Fig. 4(A)). A proportional bubble map of the raw data showed an aggregated infestation pattern with several areas of high-intensity infestation. This trend was also evident in the Inverse Distance Weighted interpolation map of percent foliar damage (Fig. 5(A)). The spatial clustering of foliar damage was significant (positive z-score and $P < 0.01$) in block 1 (Table 2).

In block 2, foliar damage was confined to certain areas of the block composed of cultivar 856 (Fig. 4(B)). The proportional bubble map and the Inverse Distance Weighted interpolation map showed the foliar damage was clustered in certain areas of the block (Figs. 4 and 5). The spatial clustering was significant (positive z-score and $P < 0.01$) based on Global Moran's Index in block 2 (Table 2). In block 3, the proportional bubble map and the Inverse Distance Weighted interpolation map suggested that foliar damaged was clustered spatially by cultivar; however, the clustering was not significant ($P = 0.03$).

3.3 Comparison of ground-based visual assessment to the sUAV-based assessment

In block 1, where macadamia felted coccid damage was greatest, regression of sUAV-based assessment of percent foliar damage against the ground-based visual observations of trees with positive levels of foliar damage had a significant positive linear correlation (F = 796.52; df = 1, 227; $P < 0.01$; $r^2 = 0.77$; Fig. 6(A)). The slope of the regression line (1.06 ± 0.04) indicated that when the foliar damage is high and visible from the top of the canopy, the estimates from ground and sUAV are similar. Regression of sUAV-based assessments of foliar damage when the ground-based assessments were between >0 and 20% also had a significant, positive linear relationship (F = 88.63; df = 1, 72; $P < 0.01$; $r^2 = 0.55$; Fig. 6(B)). The higher slope (1.92 ± 0.20) of the regression line when the ground-based assessments were between 0 and 20% suggested a higher sensitivity for UAV-based assessment for the cultivar 344 than the ground-based assessment. Similar trends were observed when the ground-based visual assessments were between >0 and 10%, but with a poorer fit,

Table 1. Mean row-wise percent foliar damage (± SE) from ground-based assessments in three macadamia blocks showing variation in the damage among rows

Row	Block 1	Block 2	Block 3
1	20.52 ± 3.7	3.78 ± 2.6	7.75 ± 2.4
2	21.92 ± 2.6	3.57 ± 2.2	5.93 ± 2.8
3	37.03 ± 4.8	6.46 ± 2.5	0.68 ± 0.5
4	30.00 ± 3.6	6.96 ± 1.7	0.00 ± 0.0
5	26.35 ± 3.4	3.82 ± 1.9	0.89 ± 0.6
6	3.38 ± 2.5	4.41 ± 1.3	5.98 ± 2.5
7	54.32 ± 4.6	2.39 ± 1.8	0.05 ± 0.1
8	46.98 ± 4.9	0.00 ± 0.0	1.66 ± 1.4
9	49.32 ± 6.6	0.00 ± 0.0	0.50 ± 0.3
10	35.65 ± 7.0	0.00 ± 0.0	2.23 ± 1.6
11	17.39 ± 4.6	0.00 ± 0.0	0.30 ± 0.2
12	0.00 ± 0.0	0.07 ± 0.1	2.70 ± 1.7
13	0.00 ± 0.0	0.07 ± 0.6	1.25 ± 1.1
14	0.91 ± 0.0	1.69 ± 0.7	
Percent damage by cultivar	**344:** 31.00 ± 1.6	**856:** 4.42 ± 0.7	**508:** 11.53 ± 1.8
	800: 0.0 ± 0.0	**333:** 0.00 ± 0.0	**333:** 0.30 ± 0.2

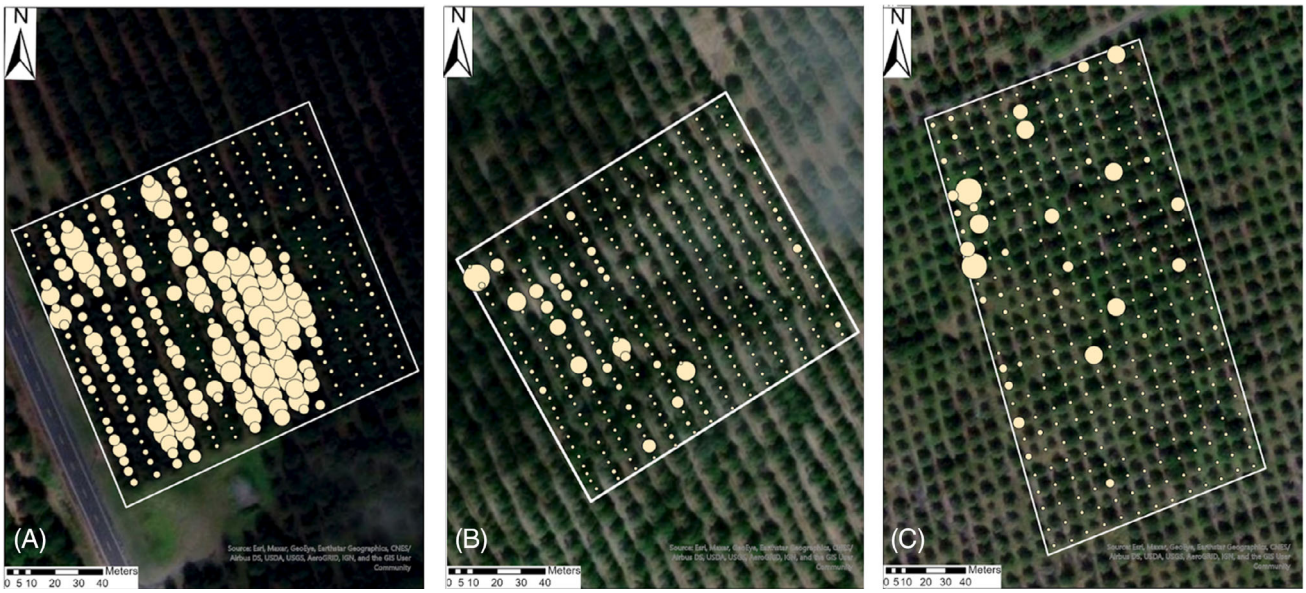

Figure 4. (A) A proportional bubble map of percent foliar damage assessed by ground-based visual observations in block 1, (B) in block 2, and (C) in block 3. The range of damage was from 0 to 90.0%, from 0 to 62.5%, and from 0 to 55%, respectively.

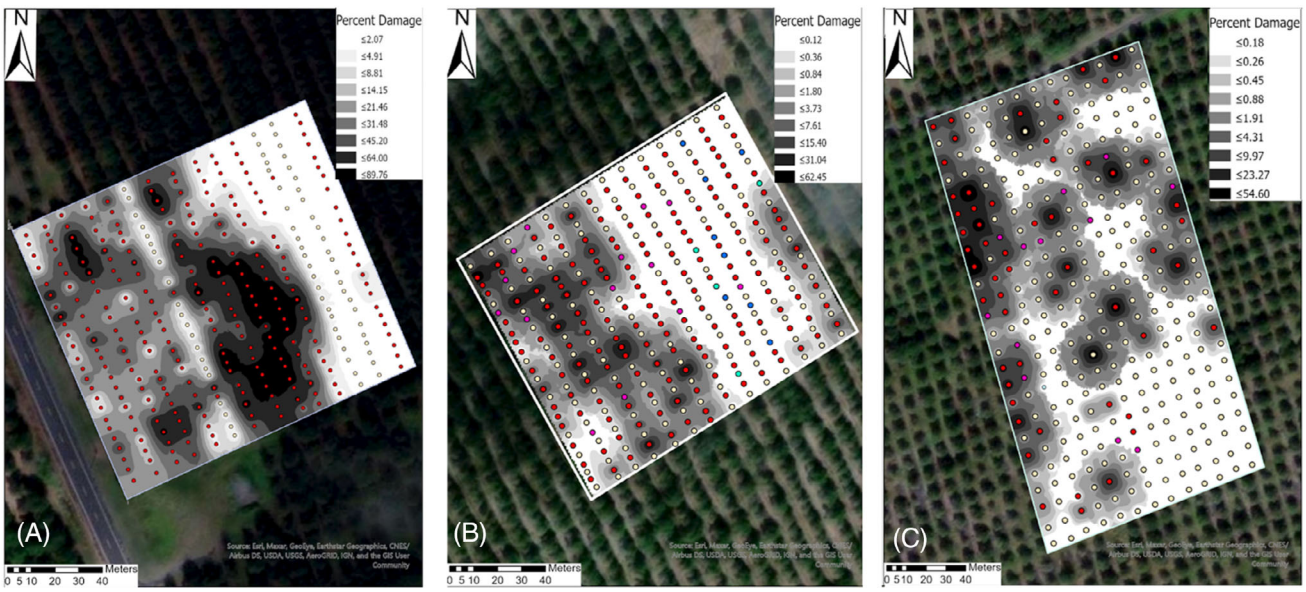

Figure 5. Inverse Distance weighted interpolation map of percent foliar damage assessed by ground-based visual observations for (A) block 1, (B) block 2, and (C) block 3.

Table 2. Spatial clustering of percent foliar damage assessed by ground-based visual observation using Global Moran's Index in three blocks of macadamia orchards in Hawaii

	Moran's Index	z-score	*P*-value
Block 1	0.72	19.13	< 0.01
Block 2	0.15	4.65	< 0.01
Block 3	0.09	2.14	= 0.03

possibly because of the smaller sample size ($F = 21.12$; $df = 1, 42$; $P < 0.01$; $r^2 = 0.33$) (Fig. 6(C)). The slope of the regression (1.18 ± 0.25) when the ground-based assessments were > 0 and 10% suggests a comparable estimate for both methods (ground and sUAV) at lower levels of damage. A total of 104 trees of both cultivars showed no signs of macadamia felted coccid damage based on visual assessment. Among these healthy trees, sUAV-based assessment classified five trees as having more than 5% foliar damage (*i.e.*, false positives), primarily due to the overlap of healthy and damaged canopies. Among the remaining healthy trees (n = 99), the mean foliar damage assessed by sUAV was only 0.2 ± 0.04%. In block 1, less than 1% (n = 229) of the trees assessed from the ground with detectable damage were classified as having no macadamia felted coccid damage by sUAV (false negatives). The mean foliar damage on these two trees was 1.25% based on ground assessment.

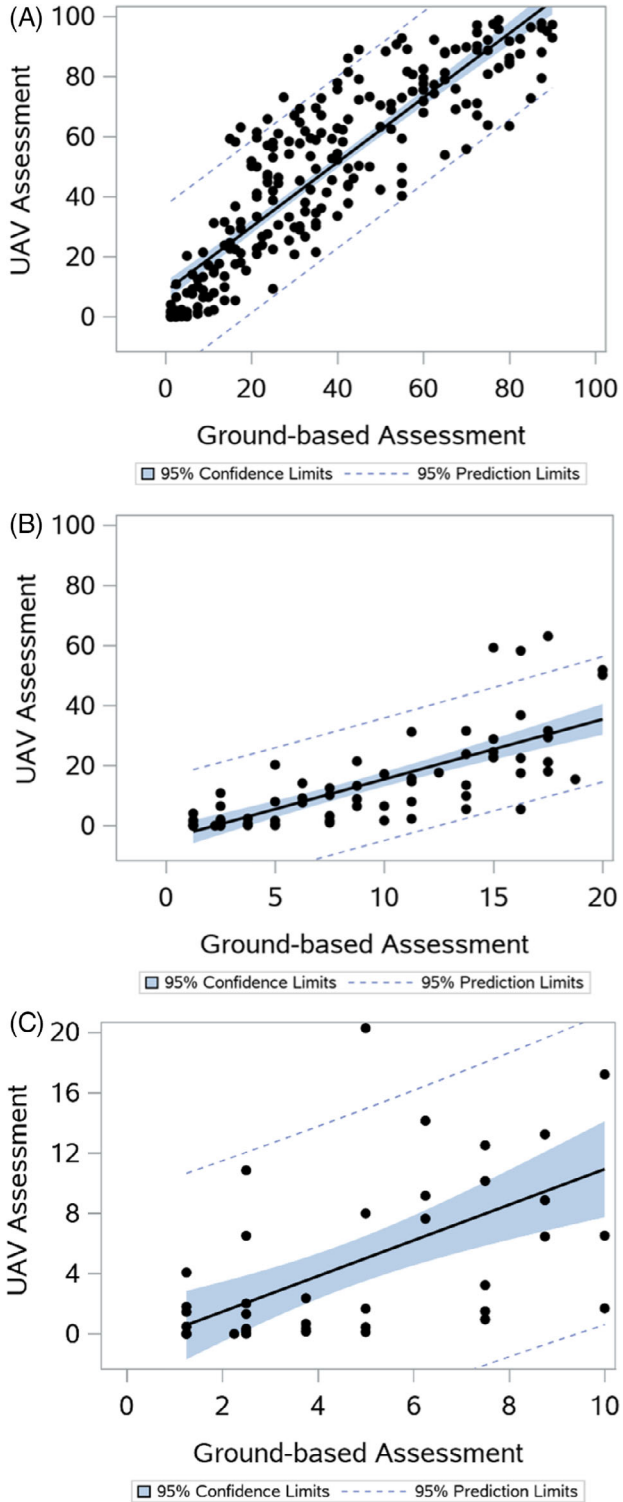

Figure 6. Regression of sUAV-based aerial assessment of percent foliar damage from macadamia felted coccid against ground-based visual assessment in block 1 (A) for all values ($P < 0.01$), (B) for points with visual damage ≤20% ($P < 0.01$), and (C) when visual damage ≤10% ($P < 0.01$).

In block 2, where the macadamia felted coccid infestation and damage was patchy, regression of sUAV-based assessments of percent foliar damage against ground-based visual observations of non-0% foliar damage also exhibited a significant linear

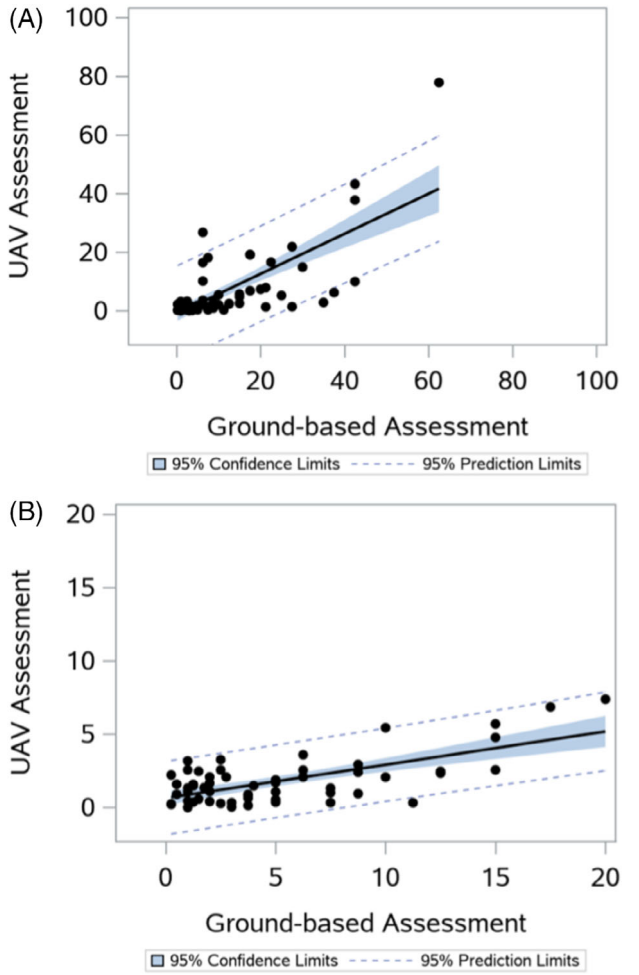

Figure 7. (A) Regression of sUAV-based aerial assessment of percent foliar damage from macadamia felted coccid against ground-based visual assessment in block 2 for all values ($P < 0.01$) and (B) for points with visual damage ≤20% ($P < 0.01$).

relationship (F = 83.17; df = 1, 73; $P < 0.01$; Fig. 7(A)). Block 2 had comparatively fewer trees with foliar damage and the range of foliar damage was lower compared to block 1. Despite these factors, the regression showed an overall level of fit of $r^2 = 0.52$ (n = 75). The linear relationship was significant (F = 44.76; df = 1, 55; $P < 0.01$) when the visual damage was below 20% (Fig. 7(B)). Slopes of the regression lines were < 1 in both cases (0.68 ± 0.07 and 0.23 ± 0.03), suggesting that the ground-based assessment was higher than the sUAV-assessment for trees of cultivar 856 that showed damage. The lower estimate from the sUAV assessment is possibly due to the spreading canopy architecture of cultivar 856 and to the position of infestations, being located primarily on lower branches, out of sight of sUAV imagery. Trees in block 2 that had no detectable macadamia felted coccid damage (n = 255) based on ground-based assessment, had a mean foliar damage (false positives) of 2.0 ± 0.3% when assessed by sUAV. Among these cases, 21 trees (primarily cultivar 333) had a false positive foliar damage rating of more than 5%. Cultivar 333 was prone to another disease, 'slow decline,' caused by *Kretzschmaria clavus*, that was prevalent in old macadamia trees.[35] Affected trees showed chlorosis, defoliation, and dead branches. Because of the high resolution of sUAV-based classification, some of this damage was likely mis-classified as pixels with macadamia

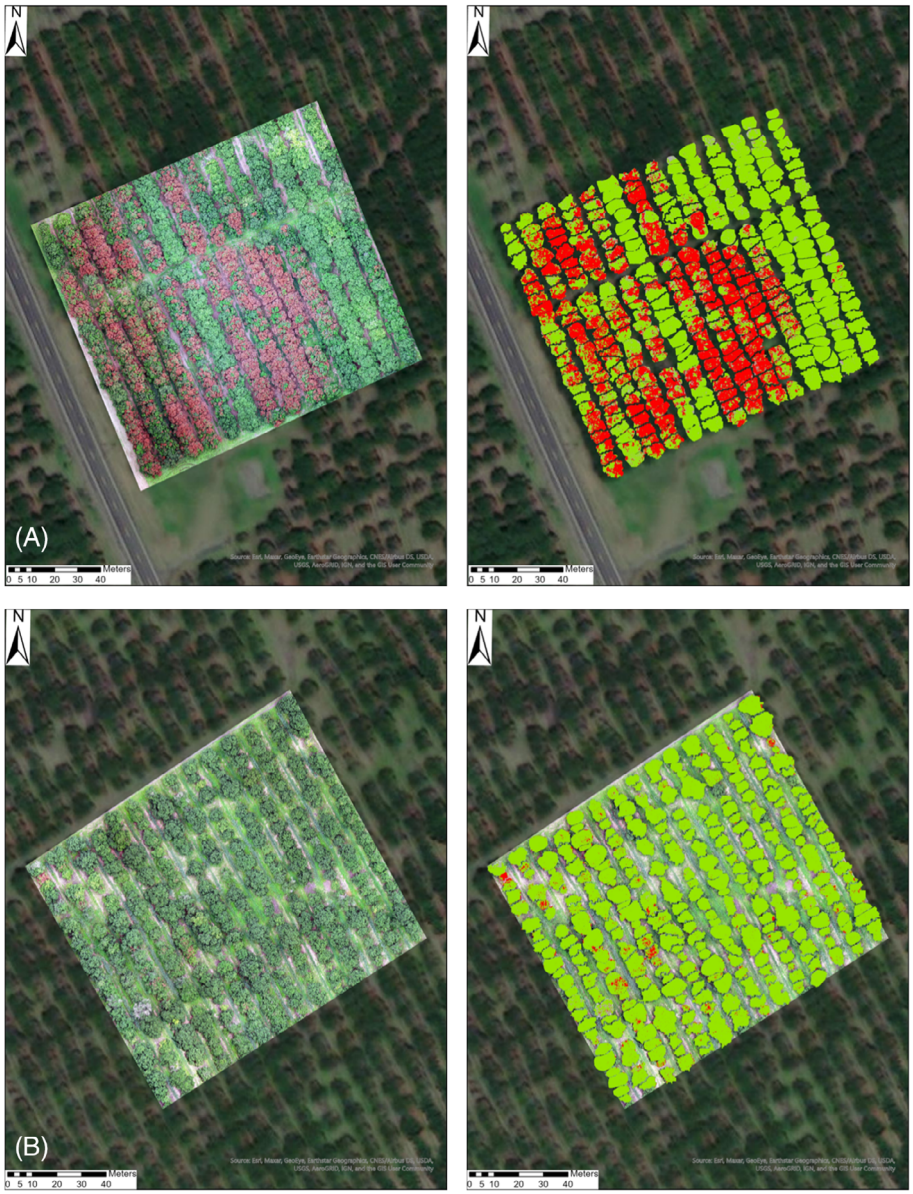

Figure 8. Orthorectified mosaics of RGB imagery and the imagery classified using the Support Vector Machine algorithm showing varying ranges of macadamia felted coccid damage in macadamia in (A) block 1 and (B) in block 2.

felted coccid damage. In block 2, out 75 trees that had some level of foliar damage based on ground assessment, one tree (1.33%) was classified as having no damage by sUAV. On this tree, ground-based assessment of foliar damage was 1%.

In block 3, there was a linear relationship between the level of foliar damage in sUAV assessments and the level seen in ground-based positive foliar damage assessments, but the relationship was not significant ($F = 5.16$; df = 1, 50; $P = 0.03$; $r^2 = 0.08$). Unlike blocks 1 and 2, the infestation in block 3 was at a stage where much of the affected foliage had already been lost and the remaining damage was masked by new growth; consequently, further comparisons were not attempted.

The location of visible infestations derived from the RGB orthomosaic and tree crown maps classified using the Support Vector Machine algorithm based on sUAV aerial imagery were both comparable to the infestation maps based on ground-based observations (Figs. 4 and 8). The Support Vector Machine algorithm-based pixel classification of the orthomosaics was sensitive enough to pick up low levels of damage in blocks 1 and 2. The contrast in infestation between susceptible and tolerant cultivars was clearly visible in the imagery from block 1, possibly because of the high infestation rate and a distinctive planting layout that allowed the cultivars to be visually distinguished.

4 DISCUSSION

Heavy infestations of sap-feeding macadamia felted coccid cause physiological stress to the macadamia trees and kill branches, resulting in a characteristic pattern of dieback with copper-colored leaves.[32] This distinct color change in the foliage from green to brown initially appeared on isolated trees in the orchard and gradually spread to other trees if macadamia felted coccid was left unchecked. Macadamia felted coccid is easily controlled by pesticide applications, often requiring only one or two

applications per year.[42] Despite being highly visual, early detection of foliar damage is primarily limited by practical difficulties associated with scouting large orchards. We investigated the feasibility of detecting the change in foliage color in orchards having varying levels of infestation using a sUAV. We mapped patterns of cultivar plantings and macadamia felted coccid infestations and damage in macadamia orchards using ground-based observation and GIS, then made sUAV-based aerial assessments of damage. Spatial analysis of ground- and sUAV-based assessments revealed differences in cultivar susceptibility to macadamia felted coccid infestation. Significant spatial clustering of foliar damage was mainly caused by groupings of cultivars susceptible to macadamia felted coccid infestation, and this pattern was observed in two blocks where there were susceptible cultivars (344 and 856) and tolerant cultivars (800 and 333). sUAV and ground-based estimates of foliar damage were similar for the cultivar 344, but for the cultivar 856 ground-based estimates of damage were higher, possibly due to the differences in canopy architecture and significant dieback initially in the lower canopy. At low foliar damage levels (10–20%), sUAV and ground truthing data were significantly positively correlated, suggesting sUAV may be useful in detecting early stages of macadamia felted coccid infestation.

Ground-based visual assessment preceded our sUAV-based assessment. In our ground-based samples, there were strong differences among cultivars in the level of macadamia felted coccid damage. Cultivars 344, 856, and 508 were highly susceptible, whereas cultivars 800 and 333 appeared to be tolerant. The strength of the tolerance was demonstrated by the differences in damage levels when tolerant and susceptible cultivars occurred side-by-side. The best example was in block 1 (Figs. 1(A) and 4(A)), where a row of the tolerant cultivar 800, which showed no damage (0%), was surrounded by five rows on either side of the susceptible cultivar 344 that showed high damage (84.4%). Cultivar susceptibility to macadamia felted coccid has important implications for orchard pest management. New and replacement plantings should use the tolerant cultivars 800 or 333 to avoid macadamia felted coccid damage. Monitoring for macadamia felted coccid could focus on susceptible cultivars, such as 344, 856, and 508, which would save time and resources and may result in higher success in detecting incipient macadamia felted coccid infestations. Macadamia felted coccid populations are typically patchy,[33] and therefore identifying macadamia felted coccid-infested patches may allow for spot spraying, which will reduce insecticide application costs as compared to spraying whole blocks which may be planted with both susceptible and tolerant cultivars. Tree age was not a factor in block 1 as both cultivars were planted at similar times. In block 2, the trees of the susceptible cultivar 856 (that had been interplanted with the tolerant cultivar 333) were of varying ages. Both young and old trees of 856 (the susceptible cultivar) were infested with the felted coccid, indicating that tree age was not factor in infestation.

Our observations on the spatial distribution of macadamia felted coccid infestations from ground-based visual assessments are in general agreement with previous research, in that patterns of infestation are primarily dictated by the planting pattern of susceptible cultivars and tree spacing. For example, in block 1, heavy foliar damage was clustered in areas where the cultivar 344 was most abundant. In blocs 2 and 3, where the susceptible cultivars were planted in an alternate tree or scattered pattern, macadamia felted coccid infestations were less aggregated. When infestations started in our blocks is unknown, but the infestations are believed to have been present for several years. At the time of our sampling, the rate of infestation was high on cultivar 344, but only moderate to low on cultivars 856 and 508. Adult females are sedentary and attached to the bark or leaves. First instar nymphs (crawlers) that emerge from the egg sacs of females often settle near their natal females, leading to clumped colonies, but some crawlers make longer dispersal movements and may reach nearby trees by crawling if canopies overlap, or may be carried further by wind.[43]

In perennial tree crops, use of drones for monitoring plant health or detection of pest incidence is still in its emergent phase. Unlike annual crops, the complex canopies of tree crops requires the development of customized processes to collect sUAV imagery suitable for the detection of pests and diseases. Previous studies using sUAV imagery discuss methodologies for differentiating spectral signatures of healthy *versus* diseased tree canopies based on various vegetation indices.[25] However, in macadamia nut orchards, macadamia felted coccid damage is easily identifiable using simple RGB imagery. This allows the use of a simplified and cost-effective workflow for surveillance and early detection of macadamia felted coccid infestation using readily available sUAV equipment and techniques. Our study also benefited from our ground-based visual assessment of macadamia felted coccid densities, which provided tree-by-tree data in each block. In many case studies involving tree crops, sUAV-based photogrammetry has primarily been used to address one or two aspects of image processing and manipulation, such as creation of a 3D point cloud of the data, canopy detection,[44] or height determination.[45] A comprehensive workflow process that integrates ground truthing with sUAV-based photogrammetry has been attempted in forest crops,[29] and sUAV-based assessment of plant stress associated with insects or diseases often employs multiple spectral bands to identify bands that exhibit highest correlation with ground data.[13] Because macadamia felted coccid-induced damage is distinct and visible in the RGB spectrum, we focused on developing a workflow process to calculate the extent of foliar damage in canopies of individual trees from simple RGB imagery. Our workflow integrated multiple image processing steps that included orthorectification of sUAV-imagery, pixel-level classification of healthy *versus* damaged foliage, generation of a 3D point cloud for the data, separation of tree canopies from the terrain and foreign vegetation, and delineation of individual tree crowns with unique identifiers. Most importantly, the process allows extraction of tree crown health data from individual trees for direct comparison with ground-based observation.

Visual assessment of foliar damage is not a widely practiced scouting method in macadamia. In this study, we opted for a ground-based visual method to generate a range of tree-level observations to compare with sUAV-based assessments. The significant agreement between ground-based visual assessments and independent sUAV-based assessments suggests that sUAV-based assessments reliably detect macadamia felted coccid-induced foliar damage, and that the method is sensitive even at low levels of foliar damage. In this study, documenting foliar damage of all the trees within each block enabled subsampling based on the degree of foliar damage. As a monitoring tool, reliable predictions are most useful if foliar damage is detectable in the infestation's early stages. Therefore, the feasibility of using sUAV as a monitoring tool will depend on its ability to detect low levels of damage. In two of our study blocks, we found a significant linear relationship between the two sampling methods when foliar damage was <20%, and a similar correlation was even observed in trees with foliar damage <10%. Detecting macadamia felted

coccid damage at low levels when it is confined to isolated trees in the orchard and applying insecticides could prevent further spread of the coccid and save the infested trees. False negative assessment by sUAV was rare and only occurred when the actual foliar damage present on trees was extremely low. Cultivar differences in canopy architecture or differences in infestation patterns (lower *versus* upper canopy, interior *versus* exterior of canopy) in different cultivars might influence the efficiency of damage detection using sUAV. The flight path, altitude, and camera tilt of the sUAV could, however, be adjusted to acquire more complete imaging in blocks that have low levels of damage or when tree canopies interfere with detecting infestations on the lower branches. Improvement is still needed in the method's capacity to identify and classify the damage when symptoms first develop, i.e., before leaves turn brown. This would require measuring foliar color at regular intervals and developing training datasets to detect damage early. Although our study aimed to provide a completely automated detection workflow, some further adjustments may be required. However, since macadamia felted coccid damage is visually identifiable with drones and the generated imagery has high resolution, users of the method could employ ground truthing surveys to lower the SUAV's rate of both false positives and negatives. Our study documents a workflow for detecting and classifying macadamia felted coccid infestation using a sUAV that can serve as the basis for further development.

The existence of heavily macadamia felted coccid-infested macadamia trees with 80–90% of foliar damage in our study (which was carried out in a commercial orchard) illustrates the difficulty in detecting macadamia felted coccid outbreaks using manual scouting and reflects the general lack of knowledge among farm managers regarding the potential harm from the pest. Currently, ground methods to quantify macadamia felted coccid in blocks the size we studied could take more than a week, including the time required to trap the crawlers on the sticky tape and count them under a microscope. Additionally, the existing ground sampling method is limited in the number of trees within each block that, as a practical matter, can be sampled, and thus the method can miss early signs of infestation in some areas. In this study we demonstrated that an sUAV can be used to detect macadamia felted coccid-damaged foliage with high accuracy even at low damage levels. Use of RGB spectral bands to detect the foliar characteristics associated with macadamia felted coccid damage is comparable to visually scouting all trees in an orchard but with the added advantage of being able to view the top of the canopy. Our study also documented clear cultivar differences in susceptibility to macadamia felted coccid. Information about the planting layout and location of susceptible cultivars in existing orchards could improve the efficiency of scouting by limiting the sUAV sampling efforts to areas where susceptible cultivars were located. Effective orchard design using tolerant cultivars as pest barriers could lead to both higher yields and more effective pest management programs. This study focused on a single point in time of a late-stage infestation. Periodic documentation of foliar color to detect changes caused by macadamia felted coccid would enable detection of early infestation. The estimated mapping rate in our study was 0.4 ha per minute, and therefore sUAV could scout thousands of macadamia trees within an hour. If an efficient workflow to process the imagery were in place, a report for the grower on the health of the trees could be generated within a few hours, leading to more efficient and effective pest management and a reduction in monitoring and pest control cost for the producer.

ACKNOWLEDGEMENTS

We thank Mr. Dan Springer, Orchard Manager of MacFarms of Hawaii for providing access to the orchards and for assistance in identifying cultivars. We thank Mr. Nathan Trump, President of Hawaii Macadamia Nut Association for his guidance and assistance in formulating this project. We are grateful to Roy Van Driesche and Angelita Acebes-Doria for reviewing an early draft of the paper. This article reports the results of research only. Mention of a proprietary product does not constitute an endorsement or a recommendation by the USDA for its use. USDA is an equal opportunity employer.

This research was supported in part by an appointment to the Agricultural Research Service (ARS) Research Participation Program administered by the Oak Ridge Institute for Science and Education (ORISE) through an interagency agreement between the U.S. Department of Energy (DOE) and the U.S. Department of Agriculture (USDA). ORISE is managed by ORAU under DOE contract number DE-SC0014664. All opinions expressed in this paper are the author's and do not necessarily reflect the policies and views of USDA, DOE, or ORAU/ORISE.

CONFLICT OF INTEREST DECLARATION

Authors do not have any conflict of interest associated with this publication.

DATA AVAILABILITY STATEMENT

The data that support the findings of this study are available from the corresponding author upon reasonable request.

REFERENCES

1 Syifa M, Park SJ and Lee CW, Detection of the pine wilt disease tree candidates for drone remote sensing using artificial intelligence techniques. *Engineering* **6**:919–926 (2020).
2 Tetila EC, Machado BB, Astolfi G, Belete NADS, Amorim WP, Roel AR *et al*., Detection and classification of soybean pests using deep learning with UAV images. *Comput Electron Agric* **179**:105836 (2020). https://doi.org/10.1016/j.compag.2020.105836.
3 Bhoi SK, Jena KK, Panda SK, Long HV, Kumar R, Subbulakshmi P *et al*., An internet of things assisted unmanned aerial vehicle based artificial intelligence model for rice pest detection. *Microprocess Microsyst* **80**:103607 (2021). https://doi.org/10.1016/j.micpro.2020.103607.
4 Huang Y, Reddy KN, Fletcher RS and Pennington D, UAV low-altitude remote sensing for precision weed management. *Weed Technol* **32**:2–6 (2017).
5 Swain KC, Suitability of low-altitude remote sensing images for estimating nitrogen treatment variations in rice cropping for precision agriculture adoption. *J Appl Remote Sens* **1**:013547 (2007). https://doi.org/10.1117/1.2824287.
6 Fengbo Y, Xinyu X, Ling Z and Zhu S, Numerical simulation and experimental verification on downwash air flow of six-rotor agricultural unmanned aerial vehicle in hover. *Int J Agric Biol Eng* **10**:41–53 (2017).
7 Mogili UR and Deepak BBVL, Review on application of drone systems in precision agriculture. *Procedia Comput Sci* **133**:502–509 (2018).
8 Hunter JE, Gannon TW, Richardson RJ, Yelverton FH and Leon RG, Integration of remote-weed mapping and an autonomous spraying unmanned aerial vehicle for site-specific weed management. *Pest Manage Sci* **76**:1386–1392 (2019).
9 Klauser F and Pauschinger D, Entrepreneurs of the air: sprayer drones as mediators of volumetric agriculture. *J Rural Stud* **84**:55–62 (2021).
10 Martel V, Johns RC, Jochems-Tanguay L, Jean F, Maltais A, Trudeau S *et al*., The use of UAS to release the egg parasitoid Trichogramma spp. (hymenoptera: Trichogrammatidae) against an agricultural and a forest pest in Canada. *J Econ Entomol* **114**:1867–1881 (2021).
11 Moses-Gonzales N, Conway H, Krompetz D, Rodriguez R, Adams CG, Baez I *et al*., The use of multiple unmanned aircraft systems as a

swarm to release sterile Mexican fruit fly (Diptera: Tephritidae) into South Texas citrus groves. *J Econ Entomol* **114**:1857–1866 (2021).
12 Lo PL, Rogers DJ, Walker JTS, Abbott BH, Vandervoet TF, Kokeny A *et al.*, Comparing deliveries of sterile codling moth (Lepidoptera: Tortricidae) by two types of unmanned aerial systems and from the ground. *J Econ Entomol* **114**:1917–1926 (2021).
13 Vanegas F, Bratanov D, Powell K, Weiss J and Gonzalez F, A novel methodology for improving plant pest surveillance in vineyards and crops using UAV-based hyperspectral and spatial data. *Sensors* **18**: 260 (2018). https://doi.org/10.3390/s18010260.
14 Luo S, Liu W, Zhang Y, Wang C, Xi X, Nie S *et al.*, Maize and soybean heights estimation from unmanned aerial vehicle (UAV) LiDAR data. *Comput Electron Agric* **182**:106005 (2021). https://doi.org/10.1016/j.compag.2021.106005.
15 Zhou J, Zhou J, Ye H, Ali ML, Nguyen HT and Chen P, Classification of soybean leaf wilting due to drought stress using UAV-based imagery. *Comput Electron Agric* **175**:105576 (2020). https://doi.org/10.1016/j.compag.2020.105576.
16 Maimaitijiang M, Sagan V, Sidike P, Hartling S, Esposito F and Fritschi FB, Soybean yield prediction from UAV using multimodal data fusion and deep learning. *Remote Sens Environ* **237**:111599 (2020). https://doi.org/10.1016/j.rse.2019.111599.
17 Silva DEE, Baio FHR, Teodoro LPR, Junior CADS, Borges RS and Teodoro PE, UAV-multispectral and vegetation indices in soybean grain yield prediction based on in situ observation. *Remote Sens Appl Soc Environ* **18**:100318 (2020). https://doi.org/10.1016/j.rsase.2020.100318.
18 Hassan M, Yang M, Rasheed A, Jin X, Xia X, Xiao Y *et al.*, Time-series multispectral indices from unmanned aerial vehicle imagery reveal senescence rate in bread wheat. *Remote Sens* **10**:809 (2018). https://doi.org/10.3390/rs10060809.
19 Su J, Liu C, Coombes M, Hu X, Wang C, Xu X *et al.*, Wheat yellow rust monitoring by learning from multispectral UAV aerial imagery. *Comput Electron Agric* **155**:157–166 (2018).
20 Fernandez-Gallego JA, Lootens P, Borra-Serrano I, Derycke V, Haesaert G, Roldán-Ruiz I *et al.*, Automatic wheat ear counting using machine learning based on RGB UAV imagery. *Plant J* **103**:1603–1613 (2020).
21 Furukawa F, Maruyama K, Saito YK and Kaneko M, Corn height estimation using UAV for yield prediction and crop monitoring, in *Unmanned Aerial Vehicle: Applications in Agriculture and Environment*, ed. by Avtar R and Watanabe T. Springer, Cham, Switzerland, pp. 51–69 (2020). https://doi.org/10.1007/978-3-030-27157-2_5.
22 Xu X, Fan L, Li Z, Meng Y, Feng H, Yang H *et al.*, Estimating leaf nitrogen content in corn based on information fusion of multiple-sensor imagery from UAV. *Remote Sens* **13**:340 (2021). https://doi.org/10.3390/rs13030340.
23 Duan T, Zheng B, Guo W, Ninomiya S, Guo Y and Chapman SC, Comparison of ground cover estimates from experiment plots in cotton, sorghum and sugarcane based on images and ortho-mosaics captured by UAV. *Funct Plant Biol* **44**:169–183 (2017).
24 Wang T, Thomasson JA, Yang C and Isakeit T, Field-region and plant-level classification of cotton root rot based on UAV remote sensing, in *ASABE Annual International Meeting*. American Society of Agricultural and Biological Engineers, Boston, MA (2019). https://doi.org/10.13031/aim.201901311.
25 Castro AID, Ehsani R, Ploetz RC, Crane JH and Buchanon S, Detection of Laurel wilt disease in avocado using low altitude aerial imaging. *PLoS One* **10**:e0124642 (2015). https://doi.org/10.1371/journal.pone.0124642.
26 Zeggada A, Stella A, Caliendo G, Melgani F, Barazzuol M, Porta NL *et al.*, Leaf development index estimation using UAV imagery for fighting apple scab, in *2017 IEEE International Geoscience and Remote Sensing Symposium (IGARSS)*. Fort Worth, TX, USA (2017). https://doi.org/10.1109/IGARSS.2017.8128336.
27 Apolo-Apolo OE, Pérez-Ruiz M, Martínez-Guanter J and Valente J, A cloud-based environment for generating yield estimation maps from apple orchards using UAV imagery and a deep learning technique. *Front Plant Sci* **11**:1086 (2020). https://doi.org/10.3389/fpls.2020.01086.
28 Dash JP, Watt MS, Pearse GD, Heaphy M and Dungey HS, Assessing very high resolution UAV imagery for monitoring forest health during a simulated disease outbreak. *ISPRS J Photogram Remote Sens* **131**:1–14 (2017).
29 Näsi R, Honkavaara E, Lyytikäinen-Saarenmaa P, Blomqvist M, Litkey P, Hakala T *et al.*, Using UAV-based photogrammetry and hyperspectral imaging for mapping bark beetle damage at tree-level. *Remote Sens* **7**:15467–15493 (2015).
30 Lehmann J, Nieberding F, Prinz T and Knoth C, Analysis of unmanned aerial system-based CIR images in forestry-a new perspective to monitor pest infestation levels. *Forests* **6**:594–612 (2015).
31 USAD-NASS, Pacific region-Hawaii macadamia nut final season estimates. https://www.nass.usda.gov/Statistics_by_State/Hawaii/Publications/Fruits_and_Nuts/072020MacNutFinal.pdf [Accessed online 3 March 2020]
32 Ironside DA, The macadamia felted coccid. *Queensl Agric J* **96**:613–616 (1978).
33 Gutierrez-Coarite R, Pulakkatu-Thodi I and Wright MG, Binomial sequential sampling plans for macadamia felted coccid (Hemiptera: Eriococcidae) infesting Hawaii macadamia orchards. *Environ Entomol* **48**:219–226 (2018).
34 Gutierrez-Coarite R, Cho AH, Mollinedo J, Pulakkatu-Thodi I and Wright MG, Macadamia felted coccid impact on macadamia nut yield in the absence of a specialized natural enemy, and economic injury levels. *Crop Prot* **139**:105378 (2021). https://doi.org/10.1016/jcropro2020105378.
35 Ko WH, Nature of slow and quick decline of macadamia trees. *Bot Stud* **50**:1–10 (2009).
36 R Core Team, *R: A Language and Environment for Statistical Computing*. R Foundation for Statistical Computing, Vienna, Austria (2020).
37 Popescu SC and Wynne RH, Seeing the trees in the forest: using Lidar and multispectral data fusion with local filtering and variable window size for estimating tree height. *Photogramm Eng Remote Sens* **70**:589–604 (2004).
38 *SAS/STAT 9.4*. SAS Institute Inc, Cary, NC (2020).
39 Reay-Jones FPF, Toews MD, Greene JK and Reeves RB, Spatial dynamics of stink bugs (Hemiptera: Pentatomidae) and associated boll injury in southeastern cotton fields. *Environ Entomol* **39**:956–969 (2010).
40 Pulakkatu-Thodi I, Reisig DD, Greene JK, FPF R-J and Toews MD, Within-field spatial distribution of stink bug (Hemiptera: Pentatomidae)-induced boll injury in commercial cotton fields of the southeastern United States. *Environ Entomol* **43**:744–752 (2014).
41 Isaaks EH and Srivastava RM, *An Introduction to Applied Geostatistics*. Oxford University Press, NY (1989).
42 Wright MG and Conant P, Pest status and management of macadamia felted coccid (Hemiptera: Eriococcidae) in Hawaii, in *South African Macadamia Growers Association Handbook*, Skukuza, South Africa. Vol. **17**, pp. 69–72 (2009).
43 Conant P, Tsuda DM, Heu RA and Teramoto K, *Macadamia felted coccid, Eriococcus ironsidei Williams. New pest advisory*. Hawaii Department of Agriculture, Honolulu, HI (2005). https://hdoa.hawaii.gov/pi/files/2013/01/npa05-01-MFC.pdf [accessed online 3 March 2022].
44 Sun G, Wang X, Yang H and Zhang X, A canopy information measurement method for modern standardized apple orchards based on UAV multimodal information. *Sensors* **20**:2985 (2020). https://doi.org/10.3390/s20102985.
45 Hobart M, Pflanz M, Weltzien C and Schirrmann M, Growth height determination of tree walls for precise monitoring in apple fruit production using UAV photogrammetry. *Remote Sens* **12**:1656 (2020). https://doi.org/10.3390/rs12101656.

